

This is a repository copy of *Assessing vermetid reefs as indicators of past sea levels in the Mediterranean*.

White Rose Research Online URL for this paper:

<https://eprints.whiterose.ac.uk/170425/>

Version: Accepted Version

Article:

Sisma-Ventura, G., Antonioli, F., Silenzi, S. et al. (9 more authors) (2020) Assessing vermetid reefs as indicators of past sea levels in the Mediterranean. *Marine Geology*. 106313. ISSN 0025-3227

<https://doi.org/10.1016/j.margeo.2020.106313>

Reuse

This article is distributed under the terms of the Creative Commons Attribution-NonCommercial-NoDerivs (CC BY-NC-ND) licence. This licence only allows you to download this work and share it with others as long as you credit the authors, but you can't change the article in any way or use it commercially. More information and the full terms of the licence here: <https://creativecommons.org/licenses/>

Takedown

If you consider content in White Rose Research Online to be in breach of UK law, please notify us by emailing eprints@whiterose.ac.uk including the URL of the record and the reason for the withdrawal request.

Assessing vermetid reefs as indicators of past sea levels in the Mediterranean

¹Sisma-Ventura, G., ²Antonioli F., ³Silenzi, S., ³Devoti, S., ⁴Montagna, P., ⁵Chemello, R.,
⁶Shemesh, A., ⁶Yam, R., ⁷Gehrels, R., ⁸Dean, S., ¹Rilov, G., ⁹Sivan, D

¹Israel Oceanographic and Limnological Research (IOLR), Haifa, Israel; ²ENEA Casaccia, Roma, Italy;
³ISPRA, Roma, Italy; ⁴ISP, CNR, Bologna, Italy; ⁵Department of Earth and Marine Sciences, Section
of Ecology, University of Palermo, Italy; ⁶Department of Earth and Planetary Sciences, Weizmann
Institute of Science, Rehovot, Israel; ⁷Department of Environment & Geography, University of York,
UK; ⁸Department of Earth Sciences, University of Pisa, Italy; ⁹Department of Maritime Civilizations,
L. Charney School of Marine Sciences, University of Haifa, Israel

Keywords: Mediterranean Sea, vermetid reefs, growth rates, bio-markers, past sea-level

Abstract

The endemic Mediterranean reef building vermetid gastropods *Dendropoma petraeum* complex (*Dendropoma* spp) and *Vermetus triquetrus* develop bio-constructions (rims) on rocky shorelines at about Mean Sea Level (MSL) and are therefore commonly used as relative sea-level (RSL) markers. In this study, we use elevations and age data of vermetid reefs to (1) re-assess the vertical uncertainties of these biological RSL indicators, and (2) evaluate the vertical growth rates along a Mediterranean east-west transect, in attempt to explain the differences found in both growth rates and uncertainties. In Israel, Differential Global Positioning System (DGPS) and laser measurements relative to the local datum show that the reef surfaces mainly occupy the upper intertidal zone with variations in elevation from $+0.51\pm0.07$ m to $+0.13\pm0.05$ m along the coast. However, in specific sites the vertical uncertainty exceeds the tidal range. In some places the local vermetid species *D. anguliferum* and *V. triquetrus* appear to alternate along the vertical rim profiles. This study documents a spatial variability of vertical growth

28 rates, ranging from $\sim 1 \text{ mm yr}^{-1}$ in Israel and Crete, to $\sim 0.1\text{-}0.2 \text{ mm yr}^{-1}$ in NW Sicily and Spain.
29 The order of magnitude of the difference in growth rates correlates with the east-west spatial
30 thermal gradient of Sea-Surface Temperature (SST). Preferential skeleton deposition of *D.*
31 *petraeum* and *V. triquetrus* measured by growth axis $\delta^{18}\text{O}$ analysis shows that most calcification
32 occurs at SST above the mean annual value. These findings indicate that vermetid reefs are a
33 site-specific RSL indicator, displaying various vertical uncertainties and inner-structure
34 complexities. Local data on the indicative range of vermetids are required when reconstructing
35 relative sea-level changes using fossil vermetids.

36

37 **1. Introduction**

38 Given its mid-latitude position and very small tidal range, the Mediterranean is potentially a
39 suitable area to reconstruct past sea-level changes with high precision and accuracy (e.g., [Sivan
40 et al., 2001; 2004; Milne and Mitrovica, 2008](#)). One of the tools used in the Mediterranean to
41 reconstruct past relative sea-level (RSL) change is based on endemic bio-markers: the coralline
42 rhodophyte, *Lithophyllum byssoides* (Lamarck) rims inhabiting the western and northern
43 Mediterranean, and the sessile, aggregative, tube-building gastropods of the genus *Dendropoma*
44 ([Laborel, 1986; Laborel et al., 1994; Laborel and Laborel-Deguen, 1996; Faivre et al., 2013](#)).
45 *Dendropoma* forms rims at the edge of vermetid reef platforms inhabiting the south and east
46 Mediterranean ([Safriel, 1975a,b; Antonioli et al., 1999; Silenzi et al., 2004; Sivan et al., 2010](#)).
47 Both species inhabit the intertidal rocky shorelines close to the Mean Sea Level (MSL).
48 *Lithophyllum* rims have been also described as sea-level bio-markers ([Laborel and Laborel-
49 Deguen, 1996](#)) along the coasts of southern France ([Laborel et al., 1994; Lambeck and Purcell,
50 2005](#)) and the Adriatic coast of Croatia ([Faivre et al., 2013; 2019](#)). In the eastern Mediterranean,

51 *Dendropoma anguliferum* (a Levant endemic formerly known as *D. petraeum*, [Templado et al,](#)
52 [2016](#)) rims studied by Safriel, ([1975a,b](#)) were used for determining vertical tectonic relative
53 land movements (e.g., [Pirazzoli et al., 1991; 1994; Morhange et al., 2006; Sivan et al., 2010](#))
54 and late Holocene relative sea-level changes ([Morhange et al., 2015; Dean et al., 2019](#)).

55 Based on radiocarbon dating of *Dendropoma cristatum* in cores along the northern
56 Sicilian coast vertical rim growth during the last 400 years was suggested to be a function of
57 RSL rise ([Antonioli et al., 1999; Silenzi et al., 2004](#)). Moreover, vertical growth of *D.*
58 *anguliferum* during the last millennium was measured in rims along the Israeli coast and used
59 for paleoceanographic reconstructions ([Sisma-Ventura et al., 2009; 2014, Bialik and Sisma-](#)
60 [Ventura, 2016](#)). These studies have shown that fast growing *Dendropoma* spp. rims provide a
61 high-resolution archive of past sea-surface conditions. For example, a sea-level low-stand was
62 reconstructed during the Crusader period by Dean et al. ([2019](#)), using down-core ¹⁴C data of
63 *Dendropoma* reefs from Israel in combination with archaeological sea-level index points. In
64 this region, *Dendropoma* reefs have high vertical growth rates (~ 1.0 mm yr⁻¹) ([Sisma-Ventura](#)
65 [et al., 2014](#)). However, a recent study by Amitai et al. ([2020](#)) reported variable vertical rim
66 growth rates across the Mediterranean, suggesting that reef growth rates may vary regionally.
67 Slow growing reefs are less likely to record abrupt changes in RSL. Regional variability is also
68 apparent in the east–west genetic differentiation of the Mediterranean *Dendropoma petraeum*,
69 comprising a complex of at least four cryptic species with non-overlapping ranges ([Templado](#)
70 [et al., 2016](#)) that has resulted from past spatial fragmentation of this genus across the
71 Mediterranean ([Calvo et al., 2009](#)).

72 Previous palaeosea-level studies applied a vertical uncertainty ranging between ±10 cm
73 and ±20 cm to sublittoral *Dendropoma* spp. rims ([Sivan et al., 2010](#) and references therein),

74 based on observations that *Dendropoma* spp must be continuously flushed by sea water (Safriel,
75 1975a,b; Laborel et al., 1994; Laborel and Laborel-Deguen, 1996; Antonioli et al., 1999; Silenzi
76 et al., 2004). However, the precision of *Dendropoma* spp. and *V. triquetrus* aggregations as sea-
77 level indicators has not been firmly established. Dean et al. (2019) determined the reef
78 functional height in the Israeli coast, as the Mean Tidal level (MTL) with uncertainty between
79 the mean high tidal level and the mean low tidal level. The Mediterranean is considered to be a
80 low-tide region, yet, the mean high and low tide of Israel (Southeast Mediterranean) still vary
81 by ~ 60 cm (Shirman, 2004; Rosen et al., 2016). Moreover, it is still not very clear how
82 environmental factors, such as water temperature and wave energy, influence rim growth, but
83 it seems that wave exposure might be important (Laborel, 1986).

84 *Vermetus triquetrus* is another reef building gastropod inhabiting the Mediterranean
85 rocky shorelines alongside *Dendropoma* (Safriel, 1975a,b). However, very little is known about
86 the vertical growth of *V. triquetrus* and its potential use as a sea-level indicator (Morhange et
87 al., 2013).

88 The main aims of this paper are to study site-specific vertical reef development to
89 improve the reliability of vermetid reefs as sea-level indicators and to better understand the
90 spatial variability of their growth rates across the Mediterranean Sea. To achieve these goals,
91 site-specific vertical growth and elevations have been studied based on radiocarbon dating and
92 depth measurements from drilled cores, collected along a Mediterranean east-west transect,
93 including Israel, Lebanon, Crete, Tunisia, Sicily and southern Spain (Fig. 1). Previously
94 published elevations and radiocarbon ages on vermetid reefs from the Israeli coast (Sivan et al.,
95 2010; Sisma-Ventura et al., 2014; Dean et al., 2019) and newly obtained data from the Galilee
96 and the Carmel coasts, north Israel, have been used to evaluate the vertical uncertainties of

97 vermetid reefs as sea-level indicators. We further explore the importance of site-specific
98 environmental factors, such as water temperature and nutrient content, on the reefs' vertical
99 growth, using a detailed growth axis $\delta^{18}\text{O}$ analysis and site-specific meteorological data, sea-
100 surface temperature (SST) and Chlorophyll a.

101

102 **2. Methods**

103 The paper combines previously published bio-construction sea-level markers (elevations and
104 radiocarbon ages) from the Israeli coast (Sivan et al., 2010; Sisma-Ventura et al., 2014; Dean
105 et al., 2019) and newly obtained data from Israel (**Table 1**), along with radiocarbon ages and
106 depth measurements from drilled cores along a Mediterranean east-west transect, including
107 Lebanon, Crete, Tunisia, Sicily and southern Spain (**Fig. 1** and **Supp. Table 1**).

108

109 ***2.1. Drilling, surveying and sampling***

110 The rims formed by the Mediterranean *Dendropoma* complex of species were drilled vertically
111 from the top of the ledges towards the rock substrate, using a pneumatic corer (with a 5 cm
112 cup). The cores were cut with a diamond-head saw and sampled vertically from the top to the
113 bottom for radiocarbon dating.

114 All previous Mediterranean studies mentioned above, including in Israel, measured the
115 elevation of the reef surface manually, relative to the present sea level (using measuring rod)
116 with corrections for local tide and atmospheric pressure at the time of measurements (Anzidei
117 et al., 2011a and b). Newly obtained drillings from Israel in the Galilee and the Carmel (Dor)
118 include measurements of the top surface of *Dendropoma* rims in each drilling point relative to
119 the local Israel Land Survey Datum (ILSD) carried out with a RTK-DGPS system (RTK Proflex

120 500) (**Table 1**). In addition, surveys were carried out in four study sites spaced over 130 km
121 along the coast, mapping the absolute elevations of reef ledges above the ILSD by first fixing
122 benchmarks in each site using DGPS. A Trimble Spectra Precision Laser survey with a digital
123 smart rod then measured the heights at multiple positions in three portions on the platforms: top
124 of the *Dendropoma* rim (if it was present) at the seaward edge of the platform, behind the rim
125 (a few cm at the rim's leeward side), and the platform center (1-3 m from the edge). The two
126 portions behind the rim tend to be the *V. triquetrus* habitat (Rilov, 2016). This high-resolution
127 spatial mapping provided the average elevations of the various portions of the reef relative to
128 present tide levels.

129 Newly obtained radiocarbon ages were measured in eight reef structures along the Galilee
130 coast, Northern Israel (**Table 1**), in sites which are characterized by multi-ledge morphologies.
131 Samples were drilled in three sites and the surface of the bio-construction or the contact with
132 the sandstone substrate were ¹⁴C dated. Three new sea-level index points were obtained from
133 two archeological coastal man-made structures containing bio-constructions of *V. triquetrus*, in
134 the flushing channel of the fishpond of Achziv, and the flushing channels of Dor, Israel (**Fig.**
135 **1**). Samples were drilled in both sites and the bio-construction above the contact with the
136 sandstone substrate was ¹⁴C dated (**Fig. 2**). This newly obtained dataset is used in this study for
137 re-assessing the vertical uncertainties of vermetid reefs.

138

139 **2.2. Radiocarbon dating**

140 *Dendropoma* spp. and *V. triquetrus* specimens were cut from the cores in slices of ~ 1 cm. They
141 were separated by mechanical brushing and sonication. The organic matter was removed by
142 washing cycles of 30% H₂O₂. Special care was taken to exclude any contamination, by

143 mechanically removing the red coralline algae cements, and by using the pristine inner shell
144 structure. Radiocarbon measurements were made at the ANSTO AMS Facility on homogenous
145 powders. The three samples overlying archaeological structures in Dor and in Achziv (Fig 1)
146 were dated in the Oxford Radiocarbon Accelerator Unit (United Kingdom). Radiocarbon
147 analyses of Mediterranean samples other than those from Israel were conducted in the
148 Radiocarbon Dating Laboratory, Australian National University, Australia. The radiocarbon
149 ages were converted into calendar years using the program Calib 7.0.1 (Stuiver and Reimer,
150 1993) and the Marine 13.14c calibration data set (Reimer et al., 2013). Basin-average reservoir
151 corrections ($\Delta R \pm R$) of 53 ± 43 and 40 ± 15 (^{14}C yr) were applied for raw ^{14}C measurements from
152 the east and west Mediterranean, respectively (Reimer and McCormac, 2002).

153

154 ***2.3 Stable isotopes analysis***

155 In order to better understand the process of *Dendropoma* spp. and *V. triquetrus* skeleton
156 deposition, detailed $\delta^{18}\text{O}_{\text{skeleton}}$ variability was measured along the growth axis of four living
157 *Dendropoma* specimens, collected from the Israeli coast (Achziv and Hazrot Yassaf). The
158 carbonate powders from the skeletons (200–250 μg , 0.4 mm drill) were dissolved in 100%
159 H_3PO_4 acid at 25°C for 24h and analyzed on a Gas Bench II connected to Finnigan MAT 252,
160 at the Weizmann Institute of Science. The results are reported relative to the VPDB standard
161 with long-term analytical precision of 0.08‰ ($\pm 1\sigma$ SD).

162 The average SST during vermetid skeleton deposition was calculated using the aragonite
163 temperature-dependent fractionation during bio-mineralization described by the Böhm et al.
164 (2000) equation:

$$165 \quad (1) \text{ T}^\circ\text{C} = 20.4 - 4.43 * (\delta^{18}\text{O}_{\text{aragonite}} - \delta^{18}\text{O}_{\text{SW}})$$

166 $\delta^{18}\text{O}_{\text{aragonite}}$ and $\delta^{18}\text{O}_{\text{SW}}$ are the isotope compositions of aragonite relative to VPDB and water
167 relative to the VSMOW standard, respectively. The Israeli coast annual average $\delta^{18}\text{O}_{\text{SW}}$ of
168 $1.6\pm 0.12\text{‰}$ (Sisma-Ventura et al., 2014) was used for all calculations.

169 Site-specific mean annual SST and Chlorophyll a were obtained from the MEDATLAS
170 II (<http://doga.ogs.trieste.it/medar/climatologies/>), and were used to study the main factors,
171 influencing site-specific growth rate of *Dendropoma* spp.

172

173 **3. Results**

174 ***3.1. Elevations of reefs in Israel***

175 Along most coasts in the Mediterranean, vermetid reefs appear as a single ledge at the edge of
176 the abrasion platform located close to MSL (**Fig. 3**). In Israel, the edge of the ledge surfaces
177 (where *Dendropoma* forms rims) was found to be slightly elevated relative to the Israel Land
178 Survey Datum (ILSD). Elevations gradually decrease southward (**Fig. 4**), averaging about
179 $+0.51\pm 0.07$ m in the northernmost part of the Israeli coast, decreasing to about $+0.3\pm 0.09$ m
180 and $+0.13\pm 0.05$ m in the central and southern coasts, respectively, therefore, occupying the
181 upper intertidal zone, with a mean maximum height of $+0.39\pm 0.05$ m (Rosen et al., 2013). The
182 areas just behind the rim and the central rock platform are a bit lower (**Fig. 4**) but the entire
183 abrasion platform is slightly elevated above MSL in the upper intertidal zone.

184 Along the northern Israeli coast, multi-ledge bio-constructions were observed in a few
185 specific sites: Akko, Hazrot Yasaf, Minet A-Ziv, Segavion Island (off Achziv) and Rosh
186 Hanikra (for locations see Fig. 1). An example of the multi ledge is seen in **Fig. 5** in Achziv,
187 where surface elevations of the reef tops vary between -0.27 m and $+0.79\pm 0.06$ m (**Fig. 6** and

188 **Table 1**), thus occupying elevations above the maximum height of the mean tide. The ledge
189 surfaces yielded ¹⁴C ages that are either modern and/or too recent to be dated with any
190 confidence considering the statistical uncertainty of the calibration and reservoir-corrected
191 range (**Table 1**). This indicates that the entire multi-ledge bio-construction has accumulated
192 approximately at the same time. Multiple ledge buildup was also observed in cores drilled from
193 the island of Segavion off Achziv in the north and along the coast of Akko (**Figs. 1** and **6**). This
194 complex reef structure was not observed south of Akko (**Fig. 1**).

195

196 ***3.2. Vermetid reefs overlying archaeological structures***

197 In two archaeological sites, Dor, Carmel coast, and Achziv, Galilee coast (**Figs. 1** and **2**), bio-
198 constructions overlying historical man-made structures related to past sea level were drilled.
199 The bio-constructions infilling the Achziv channel date to the end of the 15th century - the
200 beginning of the 16th century, (**Fig. 2** and **Table 1**). The two ages of Achziv are almost identical,
201 which strengthens their reliability. At Dor, the shells of *V. triquetrus* are dated to around the
202 mid-late 18th century. These new ages also provide new RSL index points, and confirm that the
203 structures on which the organism grew were cut and formed at an indeterminate time before the
204 dates shown in **Table 1**.

205

206 ***3.3. The vertical profiles of vermetid rims***

207 Down core profiles of the rims are typically composed of *Dendropoma* shells, but can also
208 include shells of *V. triquetrus* up to 10 cm thick as was observed along the northern Israeli coast
209 (**Fig. 7**). Here *V. triquetrus* is the main gastropod covering the back reef rocky platforms.

210 However, *V. triquetrus* can also be found alongside and without *Dendropoma* as part of the
211 rim's structure (**Figures 6 and 7**).

212

213 ***3.4. Vertical growth rates of Dendropoma from various sites along the Mediterranean***

214 The vertical profiles obtained from *Dendropoma* spp. shells, cemented by a thin layer of red
215 coralline algae, show a typical structure. All core tops were either alive or dated modern by ^{14}C
216 analysis, confirming reef growth up to present, or die-off in the last few decades. The $\delta^{13}\text{C}$
217 average composition of $0.3\pm 1.3\text{‰}$ in Table 1 is a typical value for modern *Dendropoma* shells
218 ([Sisma-Ventura et al., 2014](#)). When comparing the data around the Mediterranean sites, the
219 oldest radiocarbon ages (~ 2800 cal. yr. BP) were obtained from the *D. cristatum* cores drilled
220 in NW Sicily, while those from Spain and Israel are ~ 1400 cal. yr. BP and ~ 1000 cal. yr. BP,
221 respectively (**Fig. 8**).

222 Different rates of vertical growth were observed for *Dendropoma* spp. rims in various
223 Mediterranean sites. The results in **Fig. 8** show mostly continuous vertical growth over several
224 centuries for the cores drilled along the northern Israeli coast and in Crete, and over several
225 millennia for NW Sicily, Spain and Tunisia. Gaps in rims growth are visible in the *D.*
226 *anguliferum* cores from the Israeli coast, between 800 and 600 cal. yr. BP, and along the Sicilian
227 coast around 1500 cal. yr. BP. Available growth data are not evenly distributed across the sites.
228 The two sites that contain a relatively high amount of data are Israel and NW Sicily. The highest
229 rates were measured along the Israeli coast (average rate of 1.04 ± 0.15 mm yr $^{-1}$) compared to an
230 average rate of 0.18 ± 0.03 mm yr $^{-1}$ for NW Sicily. In the western Mediterranean, the Spanish
231 coast drillings yielded average vertical growth rates of 0.13 ± 0.09 mm yr $^{-1}$ (**Table 2**). A single
232 core from Crete provides a continuous vertical growth of 1.0 mm yr $^{-1}$ (uncertainty was not

233 calculated since there is only one core). Growth rates for samples collected along the coast of
234 Lebanon and Tunisia could not be calculated due to the limited number of available ^{14}C ages.

235

236 **3.5. Oxygen isotope analyses**

237 Samples collected along the vermetid growth axis of four living specimens in different sites (all
238 from the northern Israeli coast) yielded $\delta^{18}\text{O}$ ranging from -0.4 to 1.9‰ (Fig. 9). The growth
239 axis $\delta^{18}\text{O}$ in vermetid DP-1 (from Achziv) suggests a cyclic deposition covering two cycles
240 while those of DP-3 (from Achziv) and DP-4 (from Hazrot Yassaf) indicate a lifespan of only
241 one year. The growth axis $\delta^{18}\text{O}$ range is translated to depositional temperatures between 19 and
242 30°C, where 73% of calcification occurs above the mean annual SST of 23.5°C. An average
243 SST for deposition of $25.3 \pm 3.0^\circ\text{C}$ was calculated among the four specimens, ranging between
244 $22.5 \pm 2.7^\circ\text{C}$ in sample DP-4 (Hazrot Yassaf) and $27.5 \pm 2.5^\circ\text{C}$ in DP-2 (Achziv), indicating a
245 preferential warm water skeleton deposition. The maximum SST for deposition was close to
246 30°C, while the minimum was around 19°C.

247

248 **4. Discussion**

249 **4.1. Vermetid reefs in Israel as sea-level indicators**

250 *Dendropoma* spp. reefs have been used as a sea-level marker both in the western (Antonioni et
251 al., 1999; Silenzi et al., 2004) and eastern basins of the Mediterranean (Dean et al., 2019). These
252 studies used vertical uncertainties of ± 0.1 to ± 0.2 m and showed decimeter-scale sea-level
253 changes during the last millennium. Based on his observations in Israel, Safriel (1975a,b)
254 suggested that the rims of the Carmel coast are low intertidal bioconstructions, with living tops
255 located very close to the mean sea level.

256 Unlike previous Mediterranean studies that measured elevations manually relative to sea
257 level with corrections for tide and atmospheric pressure at the time of measurements (Anzidei
258 et al., 2011a and b), our new core elevations from Israel (including the archaeological sites) are
259 based on DGPS measurements relative to the ILSD. When using previous data, we have to bear
260 in mind that a sea-level rise of ~6 cm relative to the ILSD has been calculated by Shirman
261 (2004) for the years 1958 to 2001. Sea level has continued to rise since then and is now
262 estimated to be ~12 cm above the ILSD (Rosen et al., 2013). In addition, we provide new
263 elevation data from four sites along the coast of Israel based on Laser measurements, again,
264 relative to the ILSD.

265 Our DGPS data (relative to the ILSD) show that the abrasion platforms of the Carmel
266 coast (Shikmona and Dor) are located relatively close to MSL, but the rim tops at the seaward
267 edge of the platform are always slightly elevated above the rest of the platform surface (platform
268 center). Vermetid reef platforms vary considerably in shape and size along the Israeli coast
269 (Rilov et al 2004), but there seems to be a pattern of a general decrease in elevation southward
270 from 0.51 ± 0.07 m in the Galilee to 0.35 ± 0.09 m in the Carmel coast and to only 0.13 ± 0.05 m
271 at Palmachim (Fig. 4). In Palmachim there is no visible *D. anguliferum* rim as also mentioned
272 by Tzur and Safriel, (1978). It seems that terrace shaped multi-ledge bioconstructions are found
273 only in the Galilee coast, where the rims may develop above and slightly below the intertidal
274 zone (Figs. 5 and 6). On the Carmel coast (Shikmona and Dor/Habonim) and in places around
275 Achziv, the rims are found almost at MSL.

276 Dean et al. (2019) have used down-core ^{14}C ages of *D. anguliferum* from the Israeli coast
277 to reconstruct RSL changes during the last millennium. Previously, most of the data had been
278 obtained from cores drilled along the Carmel coast, where the top of the cores containing living

279 *Dendropoma* was considered to represent MSL. In the current study, the Dor core top has been
280 measured by DGPS yielding an elevation of +0.18 m (Table 1). Taking into account the present
281 +0.12 m estimated sea-level elevation relative to the ILSD, we can confirm that the top core is
282 about $+0.06 \pm 0.05$ m relative to present MSL. It also confirms the reliability of previous
283 elevations from the Carmel coast: Dor, Habonim, Atlit and Shikmona (Dean et al., 2019).
284 However, sea-level data that were obtained from places with multi-ledge morphologies like
285 Achziv (Fig. 5) can carry higher vertical uncertainties. In some places the modern tops of the
286 reefs vary between -0.30 m and +0.80 m relative to the ILSD (Fig. 6) and therefore, are not
287 ideal sea-level indicators.

288

289 ***4.2. Archaeological implications as a test case from Israel***

290 The new ages obtained in the current study from *V. triquetrus* overlying man-made structures
291 produce new sea-level index points, but they do not provide information on when these
292 structures were built or for how long they were used. For example, the ~400 cal. yr. BP dates
293 from Achziv (Table 1 and Fig. 2) postdate the Roman ages inferred from archaeological
294 excavations at the site (Ratzlaff et al., 2012). Some additional useful information on the pools
295 can be obtained by dating the infilling bio-constructions. The settlement of *V. triquetrus* in the
296 flushing channel of Achziv during the end of the 15th century or the beginning of the 16th century
297 corresponds with a period of rising sea level (Dean et al., 2019). The preservation of *V.*
298 *triquetrus* rims inside the channel can be explained by relatively moderate flow in the channel
299 that protected it from sea abrasion. A lack of *V. triquetrus* from the Crusader Period indicates
300 no continuing flushing of the channel during periods of low sea levels (Toker et al., 2012; Dean

301 [et al., 2019](#)). According to the RSL curve of Israel, the last time the Achziv pool was functioning
302 is therefore during periods of relatively high sea level, i.e. the Roman-Byzantine period.

303

304 ***4.3. Vertical growth as a function of temperature and wave energy***

305 *Dendropoma* rims are found in the warm waters of the southeastern and southwestern
306 Mediterranean. There are a few observations of developing rims in Corsica ([Laborel, 1986](#)) and
307 some structures in north-western Sardinia ([Chemello & Silenzi, 2011](#)). This spatial distribution
308 was described by [Antonioli et al. \(1999\)](#) suggesting that SST is a key factor regulating the rim
309 growth of *D. petraeum* across the Mediterranean. Dated cores show higher vertical growth rates
310 in the eastern Mediterranean (Crete, although based on a single core, and Israel) compared to
311 the western basin (**Fig. 8**), suggesting the importance of the water temperature as a driving
312 factor. Site-specific growth rates as a function of mean annual SST and chlorophyll-a are
313 presented in **Figure 10** (data from MEDATLAS II;
314 <http://doga.ogs.trieste.it/medar/climatologies/>), showing opposite trends: growth rate is higher
315 in the east where temperatures are high and nutrient availability is low. This implies that
316 temperature (Mediterranean gradient shown in **Figure 11**) rather than food availability is the
317 likely cause for the differences in vertical growth of *Dendropoma* rims between the eastern and
318 western Mediterranean.

319 This conclusion can also be inferred from the $\delta^{18}\text{O}$ record in the vermetid tubes, measured
320 along the growth axis of shells from the Israeli coast (**Fig. 9**). The calculated depositional
321 temperatures show that most calcification occurs in summer (between 25-30°C), while below
322 about 19 °C calcification is strongly reduced. The lower temperature ranges of the western
323 basin, varying between 14 and 26°C (**Figure 11**), support lower growth rate and possibly a

324 shorter seasonal growth period of vermetids, compared to specimens from the eastern basin
325 (temperature range of 17-31 °C), although this was not measured for single specimens from the
326 western basin. Different intrinsic growth rates might also contribute to the observed difference
327 in growth between the eastern and western Mediterranean *Dendropoma* species. The higher
328 growth rates of *D. anguliferum* along the Israeli coast therefore offers higher resolution (5-6
329 years) records of paleo-oceanographic and RSL changes (Sisma-Ventura et al., 2009; 2014;
330 Bialik and Sisma-Ventura, 2016; Dean et al., 2019).

331 The $\delta^{18}\text{O}$ record measured along the growth axis also indicates maximum calcification
332 temperatures around 30 °C, supporting the hypothesis of Rilov (2016) that the recent rapid
333 warming of the southeastern Mediterranean surface waters by ~1 °C per decade over the last 30
334 years (Ozer et al., 2016) may have contributed to the collapse and near extinction of
335 *Dendropoma* populations in the southeastern Mediterranean.

336 Our results show the development of multi-ledge bio-constructions at specific sites along
337 the northern Israeli coast with a vertical thickness of more than 1 m (Fig. 5 and 6). Radiocarbon
338 ages indicate that the entire multi-ledge bio-constructions formed over a very short time, maybe
339 because they are subjected to relatively high wave activity that continuously flushed the reefs.
340 Indeed, the nearshore waters of the northern Israeli Mediterranean coast are subjected to a high
341 degree of wave exposure. For example, based on 5510 measurements in Haifa, Rilov et al.
342 (2005) calculated that 94% had a maximum wave height of >0.5 m, and 57% had a wave height
343 of >1 m. In northern Israel wave conditions can therefore promote reef development above the
344 intertidal zone. These findings along the northern Israeli coast indicate that the *D. anguliferum*
345 reefs are a site-specific sea-level indicator, displaying variable indicative ranges. This confirms

346 earlier observations of vermetid reefs by Laborel (1986) and Rovere et al. (2015) who also
347 suggested that their vertical ranges depend on wave exposure.

348 The complex inner structure of the rims along the northern Israeli coast, at times
349 containing juxtapositions of *D. anguliferum* and *V. triquetrus* (Fig. 7), is intriguing and may
350 be partly related to high abrasion rates, again due to the high degree of wave exposure, which
351 breaks the edge of the rim. Consequently, the central part of the platform, which is inhabited by
352 *V. triquetrus* only, can become the edge fronting the sea. However, other factors such as
353 storminess and ecological impacts cannot be ruled out (Dulin et al., 2020).

354

355 5. Conclusions

356 1. Biological markers like the *Dendropoma petraeum* complex of species and *Vermetus*
357 *triquetrus* are considered reliable sea-level indicators. Previous sea-level estimates based on
358 these markers included relatively small vertical uncertainties of ± 0.1 m to ± 0.2 m. However,
359 our observations based on Differential Global Positioning System (DGPS) and laser
360 measurements relative to the ILSD, reveal that these markers are more complicated as they can
361 develop multi-ledge bio-constructions where uncertainty is larger (up to about 1 m), especially
362 in northern Israel where the platform is 40-50 cm above the ILSD. Therefore, whenever
363 vermetid reefs are used to reconstruct past RSL change, the vertical uncertainty needs to be
364 evaluated for each site based on the local structure and environmental conditions.

365 2. The rates of growth of the reefs vary by 10-fold between basins and are probably
366 environment-dependent. Water temperature is suggested to be the main factor affecting their
367 growth, with our test cases showing the fastest growth rate in summer (25-30°) and reduced

368 calcification below $\sim 19^\circ$. Different growth rates can affect the age/depth model accuracy since
369 long cores produce more samples and different length core can represent very different dating.
370 3. The *Dendropoma petraeum* complex of species can be used as a sea-level indicator based on
371 the understanding that their upper part represents the upper subtidal zone and therefore can be
372 treated as a “biological sea-level” marker. The elevations of the upper living part should be
373 measured relative to the local datum (ILSD). In almost all previously published datasets, no
374 measurements relative to the local Datum were carried out. Surveying relative to the local datum
375 should reduce the uncertainty when comparing between remote datasets. We therefore
376 recommend measuring top elevations relative to local datum rather than to arbitrary tide levels.

377

378 **Acknowledgments**

379 The current research was carried out by Dr. G. Sisma-Ventura as part of his Post Doc supported
380 by the Israel Science Foundation (ISF) grant 923/11 awarded to Professor Dorit Sivan, titled:
381 “Generating a continuous, high resolution decadal to millennial scale sea-level curve for the
382 better understanding of the driving mechanisms of environmental changes”. Platform
383 measurements were funded by the Israel Science Foundation (ISF) grant 117/10 awarded to Dr.
384 G. Rilov as well as by the Marie Curie Reintegration Grant under the EU Seventh Framework,
385 grant 247149 awarded to Dr. G. Rilov. We thank Mr. Niv David and other members of the
386 Rilov lab group for the platform measurements and drilling of the cores shown in Fig 7. WRG
387 acknowledges radiocarbon dating support from the University of Oxford Radiocarbon
388 Accelerator Unit (ref. NF/2016/1/16). Dating was also supported by the Radiocarbon Dating
389 Laboratory, Australian National University, Australia (Dr. Stewart Fallon). We also like to
390 thank Dr. Or Bialik, L. Charney School of Marine Sciences, University of Haifa, Israel, for
391 modifying Figure 11 and Ms. Noga Yoselevich, the graphic artist, the Department of Geography
392 and Environmental Studies, University of Haifa, for the figures design.

393

394

- 396 Antonioli, F., Chemello, R., Imbrota, S., Riggio, S. 1999. *Dendropoma* lower intertidal reef formations and
397 their palaeoclimatological significance, NW Sicily. *Marine Geology*, 16, 155–170.
- 398 Antonioli, F., Lo Presti, V., Rovere, A., Ferranti, L., Anzidei, M., Furlani, S., Mastronuzzi, G., Orru, E.P.,
399 Scicchitano, G., Gianmaria, S., Spampinato, R.C. Pagliarulo, R., Giacomo, D., de Sabata, E., Sansò, P.,
400 Vacchi, M., Vecchio, A. 2015. Tidal notches in Mediterranean Sea: a comprehensive analysis,
401 *Quaternary Science Reviews*, 119(1), 66–84.
- 402 Antonioli, F., Ferranti, L., Stocchi, P., Deiana, G., Lo Presti, V., Furlani, S., Marino, C. 2018. Morphometry
403 and elevation of the last interglacial tidal notches in tectonically stable coasts of the Mediterranean Sea,
404 *Earth-Science Reviews*, 185, 600–623.
- 405 Amitai, Y., Yam, R., Montagna, P., Devotic, S., Matthias L'opez Correa L.M., Shemesh, A. 2020. Spatial
406 and temporal variability in Mediterranean climate over the last millennium from vermetid isotope
407 records and CMIP5/PMIP3 models, *Global and Planetary Change*, 189, 103159.
- 408 Anzidei, M., Antonioli, F., Benini, A., Lambeck, K., Sivan, D., Serpelloni, E., Stocchi, P., 2011a. Sea level
409 change and vertical land movements since the last two millennia along the coasts of southwestern
410 Turkey and Israel. *Quaternary International*, 232, 13–20.
- 411 Anzidei, M., Antonioli, F., Lambeck, K., Benini, A., Soussi, M., Lakhdar, R., 2011b. New insights on the
412 relative sea level change during Holocene along the coasts of Tunisia and western Libya from
413 archaeological and geomorphological markers. *Quaternary International*, 232, 5–12
- 414 Bialik, M.O., Sisma-Ventura, G. 2016. Proxy-based reconstruction of surface water acidification and
415 carbonate saturation of the Levant Sea during the Anthropocene, *Anthropocene*, 16, 42–53.
- 416 Bohm, F., Joachimski, M.M., Dullo, W.C., Eisenhauer, A., Lehnert, H., Reitner, J., Worheide, G. 2000.
417 Oxygen isotope fractionation in marine aragonite of coralline sponges, *Geochim. Cosmochim. Acta*,
418 64(10), 1695–1703.
- 419 Calvo, M., Templado, J., Oliverio, M., Machordom, A. 2009. Hidden Mediterranean biodiversity:
420 molecular evidence for a cryptic species complex within the reef building vermetid gastropod
421 *Dendropoma petraeum* (Mollusca: Caenogastropoda). *Biological Journal of the Linnean Society*,
422 96, 898–912.
- 423 Chemello, R., Silenzi, S. 2011. Vermetid reefs in the Mediterranean Sea as archives of sea-level and
424 surface temperature changes. *Chemistry and Ecology*, 27(2), 121–127.
- 425 Dean, S., Horton, B.P., Evelpidou, N., Cahill, N., Spada, G., Sivan, D. 2019. Can we detect centennial sea-
426 level variations over the last three thousand years in Israeli archaeological records? *Quaternary Science*
427 *Reviews*, 210, 125–135.
- 428 Dulin, T., Avnaim-Katav, S., Bialik, M.O., Sisma-Ventura, G., Angel D. 2020. Rhodolith beds along the
429 southeastern Mediterranean inner shelf: Implications for past depositional environments, *Journal of*
430 *Marine Systems*, 201, 103241.
- 431 Faivre, S., Bakran-Petricioli, T., Horvatinčić, N., Sironić, A. 2013. Distinct phases of relative sea level
432 changes in the central Adriatic during the last 1500 years – influence of climatic variations?,
433 *Palaeogeography, Palaeoclimatology, Palaeoecology*, 369, 163–174.
- 434 Faivre, S., Bakran-Petricioli, T., Barešić, J., Horvatić, D., Macario, K. 2019. Relative sea level change and
435 climate change in the Northeastern Adriatic during last 1.5 ka (Istria, Croatia), *Quaternary Science*
436 *Reviews*, 222, 105909.
- 437 Ferranti, L., Antonioli, F., Amorosi, A., Dai Pra, G., Mastronuzzi, G., Mauz, B., Monaco, C., Orrú, P.,
438 Pappalardo, M., Radtke, U., Renda, P., Romano, P., Sansò, P., Verrubbi, V. 2006. Elevation of the

439 Last Interglacial highstand in Sicily (Italy): a benchmark of coastal tectonics. *Quaternary International*,
440 145–146, 30–54.

441 Laborel, J. 1986. Vermetid Gastropods as Sea-level Indicators. In: van de Plassche, O. (Ed.), *Sea-Level*
442 *Research: A Manual for the Collection and Evaluation of Data*. Geo Books, Norwich, Amsterdam, pp.
443 281–310.

444 Laborel, J., Morhange, C., Lafont, R., Le Campion, J., Laborel-Deguen, F., Sartoretto, S. 1994. Biological
445 evidence of sea-level rise during the last 4500 years on the rocky coasts of continental southwestern
446 France and Corsica. *Marine Geology*, 120, 203–223.

447 Laborel, J., Laborel-Deguen, F. 1996. Biological indicators of Holocene sea-level and climatic variations
448 on rocky coasts of tropical and subtropical regions. *Quaternary International*, 31, 53–60.

449 Lambeck, K., Purcell, A. 2005. Sea-level change in the Mediterranean Sea since the LGM: model
450 predictions for tectonically stable areas. *Quaternary Science Reviews*, 24, 1969–1988.

451 Lambeck, K., Antonioli, F., Purcell, A., Silenzi, S. 2004. Sea-level change along the Italian coast for the
452 past 10,000 yr. *Quaternary Science Reviews*, 23, 1567–1598.

453 Milne, G.A., Mitrovica, J.X. 2008. Searching for eustasy in deglacial sea-level histories. *Quaternary*
454 *Science Reviews*, 27, 2292–2302.

455 Morhange, C., Pirazzoli, P.A., Marriner, N., Montaggioni, L.F., Nammour, T. 2006. Late Holocene relative
456 sea-level changes in Lebanon, Eastern Mediterranean. *Marine Geology*, 230, 99–114.

457 Morhange, C., Marriner, N., Excoffon, P., Bonnet, S., Flaux, C., Zibrowius, H., Goiran, J., Amouri, M.E.
458 2013. Relative sea-level changes during Roman times in the northwest Mediterranean: the 1st century
459 AD fish tank of Forum Julii, Fréjus, France. *Geoarchaeology*, 28(4), 363–372.

460 Morhange C., Marriner N. 2015. Archeological and biological relative sea-level indicators, In: Shennan I.,
461 Long A. J., Horton B. P. (eds), “*Handbook of Sea Level Research*” Wiley, Chap. 9, pp. 146–156

462 Ozer, T., Gertman, I., Kress, N., Silverman J., Herut, B. 2016. Interannual thermohaline (1979–2014) and
463 nutrient (2002–2014) dynamics in the Levantine surface and intermediate water masses, SE
464 Mediterranean Sea. *Global Planetary Change*, 151: 60–67.

465 Pirazzoli, P.A., Laborel, J., Saliège, J.F., Erol, O., Kayan, I., Person, A. 1991. Holocene raised shorelines
466 on the Hatay coasts (Turkey: paleoecological and tectonic implications). *Marine Geology*. 96, 295–
467 311.

468 Pirazzoli, P.A., Stiros, S.C., Arnold, M., Laborel, J., Laborel-Deguen, F., Papageorgiou, S. 1994. Episodic
469 uplift deduced from Holocene shorelines in the Perachora Peninsula, Corinth area, Greece.
470 *Tectonophysics*, 229, 201–209.

471 Ratzlaff, A., Yassur-Landau, A., Davies, G. 2012. Excavation at Tel Achziv 2012 Season (Archaeological
472 Report (Preliminary) No. G-10/2012). University of Haifa/Israel Antiquities Authority, Haifa.

473 Reimer P.J., McCormac, F.G. 2002. Marine radiocarbon reservoir corrections for the Mediterranean and
474 Aegean Seas. *Radiocarbon*, 44, 159–166.

475 Reimer, P.J., Bard, E., Bayliss, A., Beck, J.W., Blackwell, P.G., Bronk Ramsey, C., Buck, C.E., Cheng, H.,
476 Edwards, R.L., Friedrich, M., Grootes, P.M., Guilderson, T.P., Haflidason, H., Hajdas, I., Hatte, C.,
477 Heaton, T.J., Hoffmann, D.L., Hogg, A.G., Hughen, K.A., Kaiser, K.F., Kromer, B., Manning, S.W.,
478 Niu, M., Reimer, R.W., Richards, D.A., Scott, E.M., Southon, J.R., Staff, R.A., Turney, C.S.M., van
479 der Plicht, J. 2013. IntCal13 and Marine13 radiocarbon age calibration curves 0–50,000 years cal BP.
480 *Radiocarbon*, 55(4), 1869–1887.

481 Rilov, G., Benayahu, Y., Gasith, A. 2004. Prolonged lag in population outbreak of an invasive mussel: a
482 shifting-habitat model. *Biological Invasions*, 6(3), 347–364.

483 Rilov, G., Gasith, A., Benayahu, Y. 2005. Effect of disturbance on foraging: whelk activity
484 on wave-exposed rocky shores with minimal tidal range. *Marine Biology*, 147, 421–428.

485 Rilov, G. 2016. Multi-species collapses at the warm edge of a warming sea. *Science Reports*, 6, 36897

486 Rosen, S. D., Raskin, L., Galanti, B. 2013. Long-term characteristics of sea level, wave, wind and current
487 at central Mediterranean coast of Israel from 20 years of data at GLOSS station 80 - Hadera. Paper
488 presented at the 40th CIESM Congress, Marseille.

489 Rovere, A., Antonioli, F., Bianchi, C.N. 2015. Fixed Biological Indicators. In: Shennan, I., Long, A.J.,
490 Horton, B.P. (Eds.), *Handbook of Sea Level Research*. Wiley, pp. 268–280.

491 Safriel, U.N. 1975a. Vermetid Gastropods and Intertidal Reefs in Israel and Bermuda. *Science*, 186
492 (4169), 1113–1115.

493 Safriel, U.N. 1975b. The role of vermetid gastropods in the formation of Mediterranean and Atlantic reefs.
494 *Oecologia*, 20, 85–101.

495 Shirman, B., 2004. East Mediterranean sea level changes over the period 1958-2001. *Israel Journal of*
496 *Earth Sciences*, 53, 1–12

497 Silenzi, S., Antonioli, F., Chemello, R. 2004. A new marker for sea surface temperature trend during the
498 last centuries in temperate areas: Vermetid reef. *Global and Planetary Change*, 40, 105–114.

499 Sisma-Ventura, G., Guzman, B., Yam, R., Fine, M., Shemesh, A. 2009. The reef builder gastropod
500 *Dendropoma petraeum* - A proxy of short and long term climatic events in the Eastern Mediterranean.
501 *Geochimica et Cosmochimica Acta*, 73, 4376–4383.

502 Sisma-Ventura, G Yam, R., Shemesh, A. 2014. Recent unprecedented warming and oligotrophy of the
503 eastern Mediterranean Sea within the last millennium, *Geophysical Research Letters*,
504 DOI: 10.1002/2014GL060393.

505 Sisma-Ventura, G., Sivan, D., Steinberg, G., Bialik, O.M., Greenbaum, N. 2017. Last interglacial sea level
506 high-stands, deduced from abrasive notches, exposed at the Galilee coast, Israel. *Palaeogeography,*
507 *Palaeoclimatology, Palaeoecology*, 470, 1–10.

508 Sivan, D., Wdowinski, S., Lambeck, K., Galili, E., Raban, A. 2001. Holocene sea-level changes along the
509 Mediterranean coast of Israel, based on archaeological observations and numerical model.
510 *Palaeogeography, Palaeoclimatology, Palaeoecology*, 167, 101–117.

511 Sivan, D., Lambeck, K., Toueg, R., Raban, A., Porath, Y., Shirman, B. 2004. Ancient coastal wells of
512 Caesarea Maritima, Israel, an indicator for sea level changes during the last 2000 years. *Earth and*
513 *Planetary Science Letters*, 222, 315–330.

514 Sivan, D., Schattner, U., Morhange, C., Boaretto, E. 2010. What can a sessile mollusk tell about the
515 Neotectonics of EasternMediterranean? *Earth and Planetary Science Letters*, 296(3–4), 451–458.

516 Sivan, D., Sisma-Ventura, G., Greenbaum, N., Bialik, O.M., Williams, F.H., Tamisiea, M.E., Rohling, E.J.,
517 Frumkin, A., Avnaim-Katav, S., Shtienberg, G., Stein, M. 2016. East Mediterranean Sea levels through
518 the last interglacial from a coastal-marine sequence in northern Israel. *Quaternary Science Reviews*,
519 145, 204–225.

520 Stuiver, M., Reimer, P.J. 1993. Extended ¹⁴C data base and revised CALIB 3.0 ¹⁴C age calibration program.
521 *Radiocarbon*, 35, 215–230.

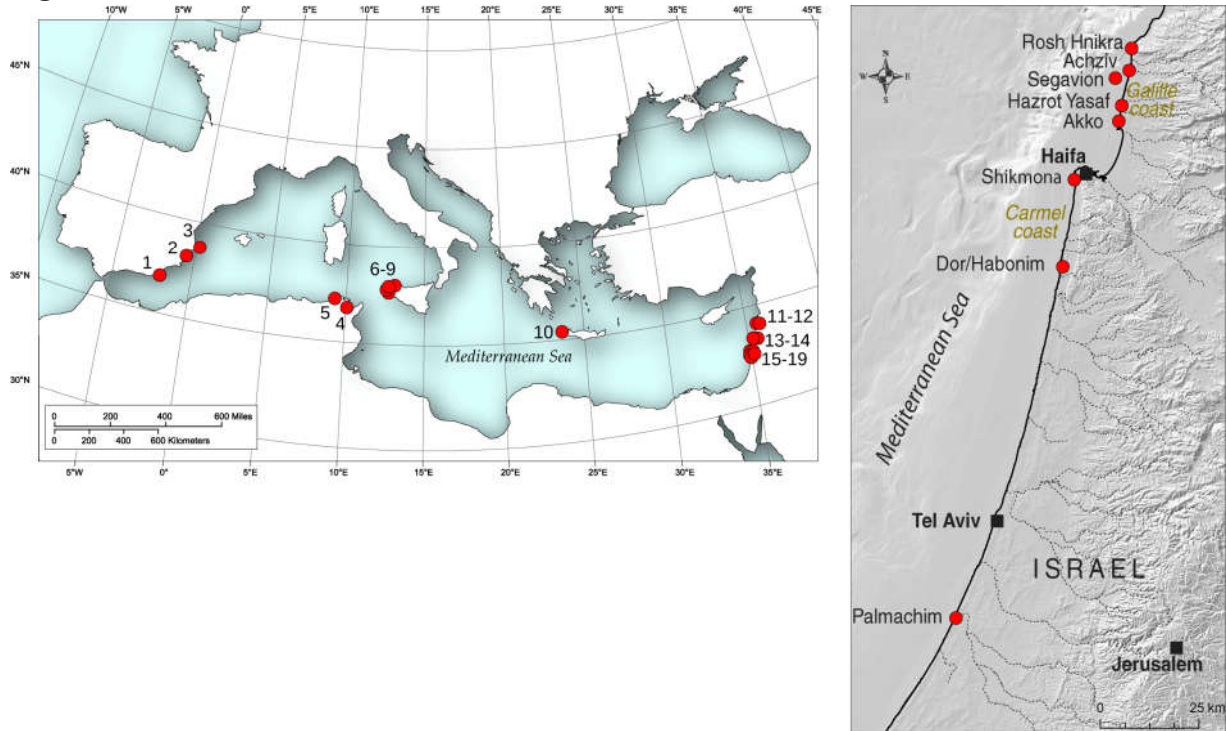
522 Templado, J., Richter, A., Calvo, M. 2016. Reef building Mediterranean vermetid gastropods: disentangling
523 the *Dendropoma petraeum* species complex. *Mediterranean Marine Science*, 17, 13–31.

524 Toker, E., Sivan, D., Stern, E., Shirman, B., Tsimplis, M., Spada, G. 2012. Evidence for centennial scale
525 sea level variability during the Medieval Climate Optimum (Crusader Period) in Israel, eastern
526 Mediterranean. *Earth and Planetary Science Letters*, 315–316, 51–6.

527 Tzur, Y., Safriel, U.N. 1978. Vermetid platforms as indicators of coastal movement. Israel Journal of
528 Earth Sciences, 124–127.

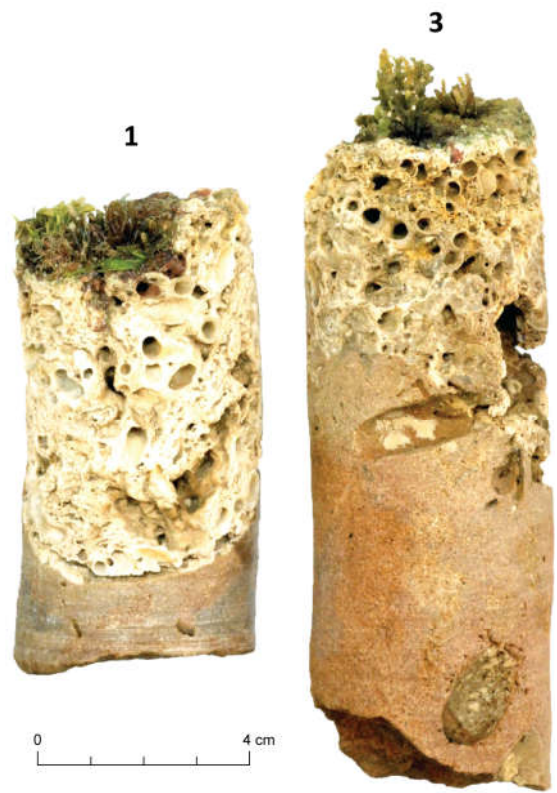
529

530 **Figures**



531

532 **Fig. 1.** Study-site maps: the numbers describe the drilling sites of *Dendropoma petraeum* complex
533 (a) along a Mediterranean West-East transect and (b) along the Israeli coast, including site-specific
534 DGPS and laser mapping.



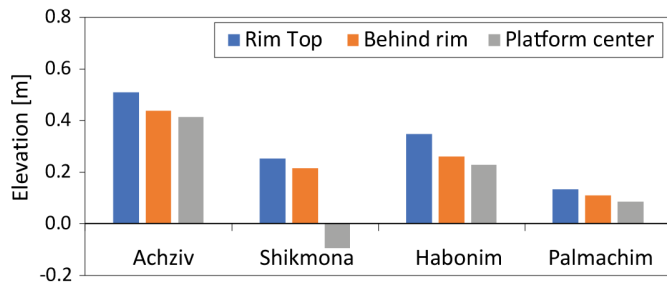
535
536
537

Fig. 2. Drilling positions of bio-constructions and retrieved cores of *V. triquetrus* infilling the flushing channel of the fishpond in Achziv.



538
 539
 540
 541

Fig. 3. Photos of vermetid reefs and drill holes showing the different morphologies of *Dendropoma* spp. rims at our study sites: (a-b) are from Spain (c-d) are from NW Sicily, (e-f) are from Create and (g-h) are from Israel.

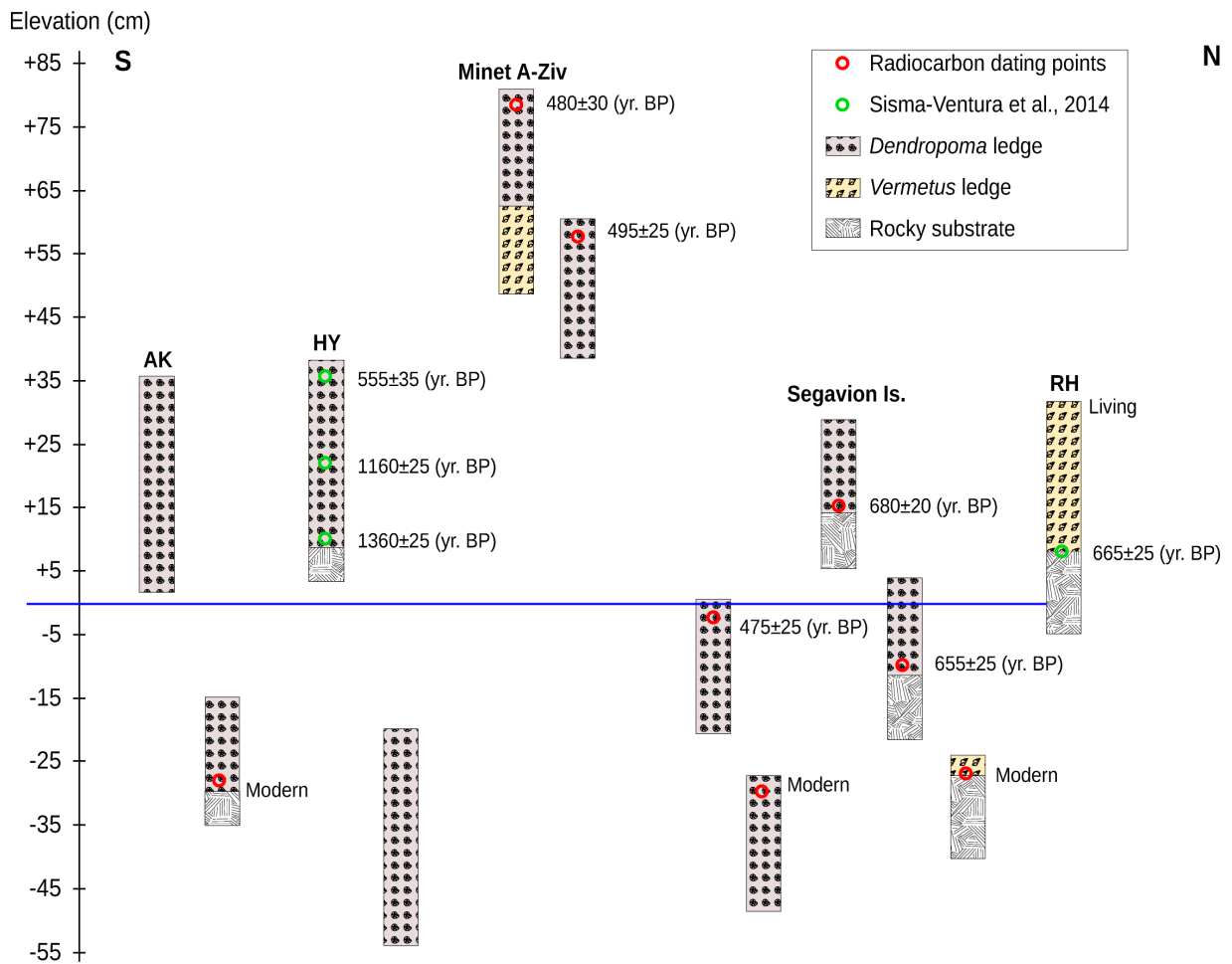


542
 543 **Fig. 4.** Site-specific DGPS and laser mean elevations of four reef sites along the Israeli coast:
 544 Achziv, Shikmona, Habonim-Dor, Palmachim, and the three studied vertical zones: top of the rim,
 545 bottom of the rim on the leeward side (behind rim), and the platform center. Measurements relative
 546 to the Israel Land Survey Datum (ILSD).

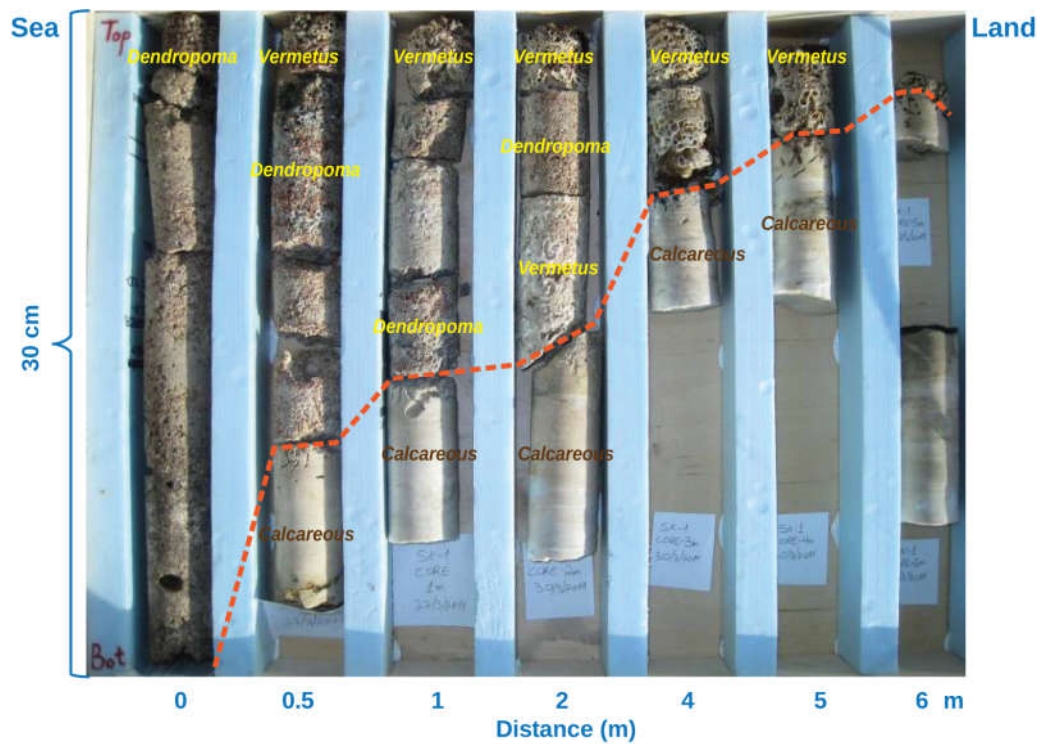
547



548
 549 **Fig. 5.** The Achziv coast multi-ledge bio-constructions during low tide showing three exposed
 550 ledges. There are two more submerged ledges. The entire structure occupying a vertical thickness
 551 of more than 1 m.

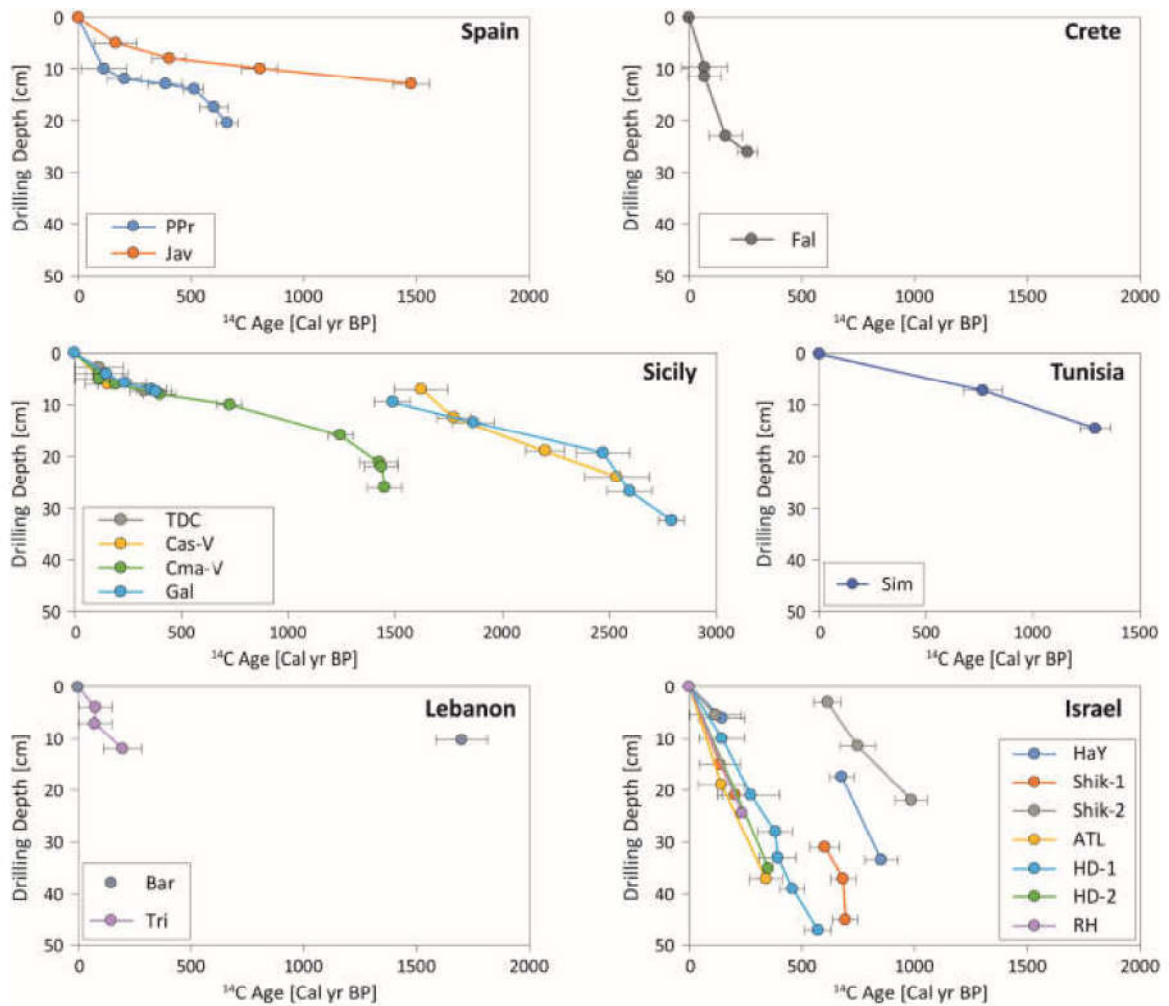


552
 553 **Fig. 6.** An illustration showing the relative vertical and temporal (^{14}C age) locations of the multi-
 554 ledge bio-constructions along the Galilee coast, north Israel; Ak is Akko, HY is Hazrot Yasaf, Rh
 555 is Rosh Hanikra (See **Figure 1**). The ledges also present the interplay between the two reef building
 556 gastropods *D. anguliferum* and *V. triquetrus*.

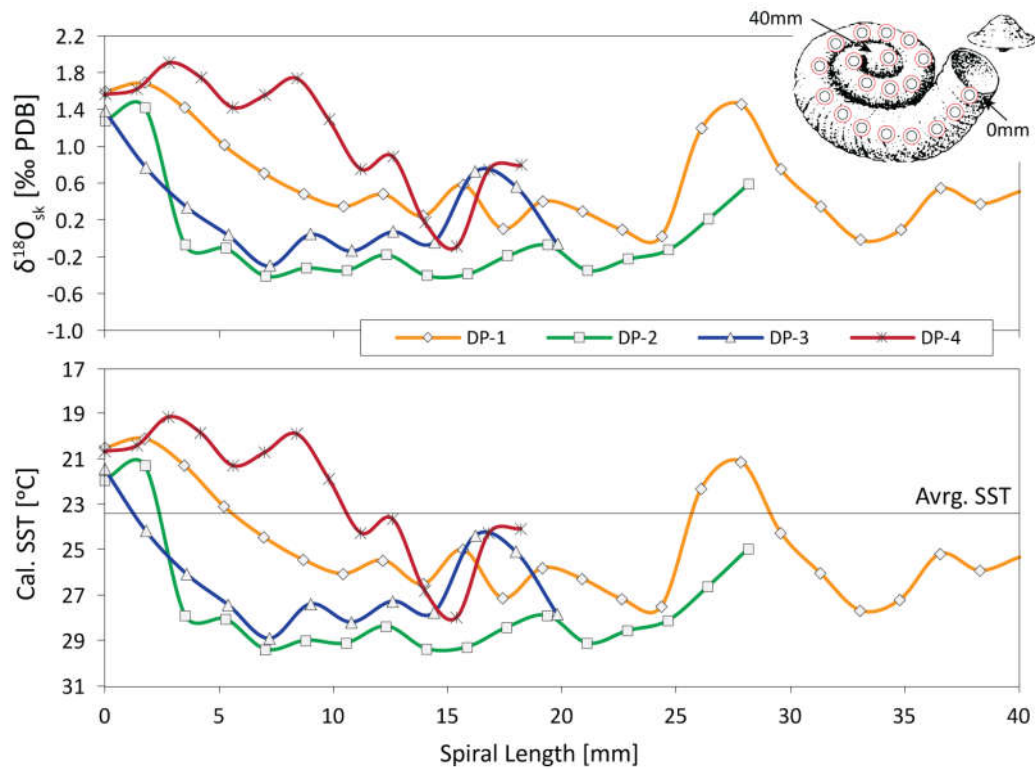


557

558 **Fig. 7.** Horizontal and vertical alternations of *V. triquetrus* and *D. anguliferum*, Shikmona, Israel
 559 (**Fig. 1**), in a series of cores perpendicular to the shore presenting the transition from *Dendropoma*
 560 to *Vermetus* and shallowing of the biogenic crust from the edge to the back of the reef.

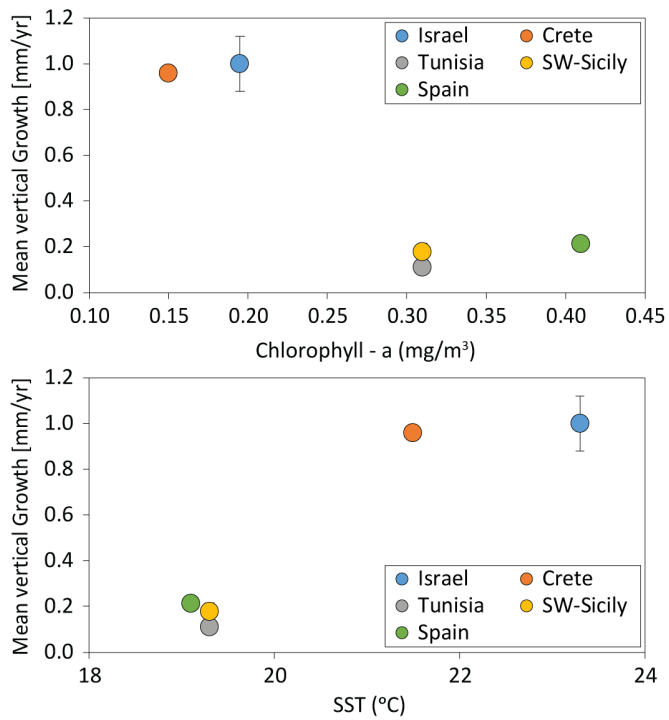


561
 562 **Fig. 8.** Vertical growth rates (drilling depth vs. ¹⁴C age) of vermetid reefs along a Mediterranean
 563 west-east transect. All data, except from Israel (Sisma-Ventura, 2014), are newly obtained and
 564 presented for the first time in the current paper. The vermetids of the western basin show older
 565 ages, but relatively low rates, compared to the much younger ages and higher growth rates in the
 566 eastern basin.



567
 568
 569
 570
 571
 572

Fig. 9. Growth axis $\delta^{18}\text{O}$ analysis and calculated SST of deposition in four *Dendropoma* samples from the Israeli coast; samples DP-1, 2 and 3 are from Achziv and DP-4 from Hazrot Yassaf. The data presented show preferential skeleton deposition in warm water.



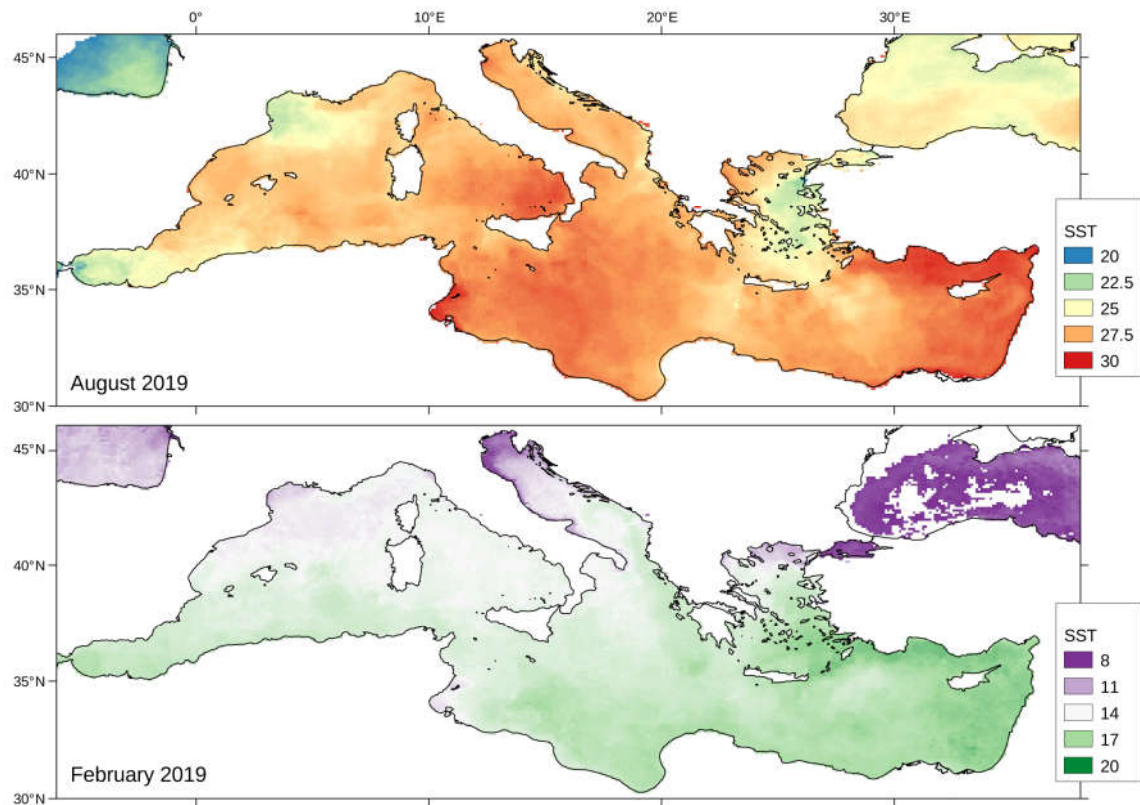
573

574

575

576

Fig. 10. Site-specific growth rates as a function of mean annual sea surface temperature and chlorophyll-a (data from MEDATLAS) showing that temperature is likely the key factor regulating the vertical growth of the different *Dendropoma* species in the Mediterranean.



577
 578 **Fig. 11.** Average SST of the Mediterranean. The data from MODIS (Moderate Resolution Imaging
 579 Spectroradiometer Satellite) represents two seasons in the Mediterranean: August, which is the
 580 warmest month and February, the coldest month. The east side of the Mediterranean is always
 581 warmer, which may explain the higher growth rates in the east relative to the west.

582

583

584 **Tables**

585

586 Table 1. New core elevations and ages from Israel. DRC refers to *Dendropoma*/Rock Contact and
 587 n.m. refers to “no measurements”

588

Location	Sp.	Sample	Elevation DGPS [m]	Sampling depth [cm]	$\delta^{13}\text{C}$ [‰ VPDB]	^{14}C ages yr. BP	Calib. BP [2 σ]	Median	Calib. AD
Achziv S channel core 1	<i>V. triquetrus</i>	OxA-34573	0.44	DRC	2.0	868±25	324 - 520	422 [±98]	1528 [±98]
Achziv N channel core 3	<i>V. triquetrus</i>	OxA-34574	0.43	DRC	2.1	888±25	334 - 538	436 [±102]	1514 [±102]
Tel Dor N Bay Ramp	<i>V. triquetrus</i>	OxA-34575	0.18	DRC	0.75	595±21	48-277	163[±102]	1788[±102]
Minat A-ziv	<i>Dendropoma</i> sp.	MA-1	0.79	7	-0.8	480	< Cal range		
	<i>Dendropoma</i> sp.	MA-2	0.6	6	-0.7	495	< Cal range		

	Dendropoma sp.	MA-4	0.03	5	-0.9	470	< Cal range		
	Dendropoma sp.	MA-5	-0.27	7	-1.0	Modern			
Segavion Island	Dendropoma sp.	SI-1B (AC-1B)	n.m.	11.5	1.2	680±35	146-399	273	1677
	Dendropoma sp.	SI-2B (AC-2B)	n.m.	6	1.8	655±25	143-325	234	1716
	V. triquetrus	SI-3B (AC-3B)	n.m.	3	-0.5	Modern			
Akko	Dendropoma sp.	AK-4-B	-0.13	11	-0.3	Modern			

589

590 Table 2. Growth rates of the bio-constructions in specific sites across the Mediterranean surveyed
591 in the current study. Calculations excluded short-cores who had 2 data points or less

592

Basin	Site	Growth rates		
		name	code	mm yr ⁻¹
West	Spain	Cabo de Gata, Playazo	CdG	0.09
		Punta Prima, Alicante	PPr	0.23
		Javea	Jav	0.08
		Avg.		0.13[±0.09]
	Italy	Capo Gallo, Palermo – upper part	Gal	0.19
		Lower part		0.16
		Castelluzzo, S. Vito	Cas V1	0.18
		Cala Mancina, S. Vito	CMa V3	0.14
		Tonnara del Cofano, S. Vito	TDC	0.23
	Avg.		0.18[±0.03]	
Tunisia	Sidi Mechrhig	SIM	0.11	
East	Greece	Falasarna, Crete	Fal	1.0
	Israel	Shikmona - 1	Shik	1.04
		Shikmona - 2		1.22
		Atlit	Atl	1.08
		Hof Dor	HD	0.84
	Avg.		1.04[±0.15]	

593

594

595

596

597

598

599

600

601

602

603 **Supplement Table 1:** radiocarbon ages and depth data from drilled cores of *Dendropoma*, taken
604 along a Mediterranean east-west transect, including Israel, Lebanon, Crete, Tunisia, Sicily and
605 southern Spain. Previously published data, marked by the symbol [*] are from Amitai et al., (2020).
606

	Site	Lab code	Drilling depth [cm]	$\delta^{13}\text{C}$ [‰ VPDB]	^{14}C activity [pMC]	^{14}C Age [yr. BP]	Cal. Range [2 σ cal. BP]	Cal. Age BP
Spain	*Punta Prima Alicante,	PPr -30	3	0.2	106.3	Modern		
		PPr -54	54	0.9	98.6	120±30	< Cal range	
		PPr -100	10	0.0	93.5	540±20	1-228	115
		PPr -120	12	2.6	92.6	620±20	132-279	206
		PPr -130	13	-1.9	88.9	800±20	313-463	388
		PPr -140	14	-1.1	90.5	950±20	469-556	513
		PPr -175	17.5	-1.0	87.4	1080±30	540-662	601
		PPr -204	20.4	1.9	86.8	1140±20	612-710	661
	*Cabo de Palos Playazo	CdGv4-53	5.3	4.8	94.9	425±30	< Cal range	
		CdGv4-110	11	3.7	93.5	540±25	1-228	115
		CdGv2-135	13.5	1.2	93.0	580±25	62-263	163
	*Javea	Jav -50	5	-0.1	93.0	580±20	72-259	166
		Jav -80	8	0.7	90.3	820±20	329-479	404
		Jav -100	10	0.2	85.0	1300±20	725-885	805
		Jav -130	13	0.2	78.2	1980±20	1396-1555	1476
	NW Sicily	*Cala Mancina, S. Vito	CMA-v3-20	2	-1.8	107.4	Modern	
CMA-v3-30			3	-0.6	94.9	420±20	< Cal range	
CMA-v3-40			4	-1.0	93.5	540±20	1-228	115
CMA-v3-50			5	3.7	93.5	540±20	1-228	115
CMA-v3-60			6	5.1	92.8	600±20	108-271	190
CMA-v3-80			8	4.2	90.4	810±20	320-472	396
CMA-v3-100			10	3.7	85.8	1230±20	665-782	724
CMA-v3-160			16	2.8	80.5	1740±20	1184-1300	1242
CMA-v3-212			21.2	0.9	78.8	1915±25	1334-1508	1421
CMA-v3-220c			22	2.7	78.7	1930±20	1354-1513	1434
CMA-v3-260		26	-2.4	78.5	1950	1367-1531	1449	
*Castelluzzo S. Vito,		CAS V1-40		0.56	101.1	Modern		
		CAS V1-50			97.4	210±20	< Cal range	
		CAS V1-60	6	4.5	93.2	570±35	48-260	154
		CAS V1-70	7		77.1	2085±45	1493-1743	1618
		CAS V1-125	12.5	2.5	75.8	2220±20	1693-1851	1772
		CAS V1-190	19	-4.3	72.7	2560±20	2106-2288	2197
		CAS V1-240	24	-1.8	70.2	2840±40	2382-2687	2535
Capo Gallo, Palermo,		GAL-10	1	1.5	108.5	>Modern		
		GAL-15	1.5	-5.7	98.9	90±20	< Cal range	
		GAL-30	3		95.5	370±30	< Cal range	

		GAL-40	4	-4.7	93.3	560±20	51-249	150
		GAL-58	5.8		92.2	660±30	134-332	233
		GAL-70	7	0.1	91.0	760±20	290-428	359
		GAL-75	7.5	-1.6	90.7	790±20	307-455	381
		GAL-95	9.5	-5.8	78.1	1990±20	1402-1569	1486
		GAL-135	13.5		75.1	2300±30	1765-1961	1863
		GAL-194	19.4	-1.6	70.6	2790±20	2345-2595	2470
		GAL-267	26.7	-1.4	69.9	2880±20	2488-2697	2593
		GAL-323	32.3	-3.4	68.3	3060±20	2728-2848	2788
	Tonnara del Cofano S. Vito,	TDC-27	2.7	0.41	93.5	540±20	1-228	115
		TDC-36	0.6	0.68	92.8	600±20	108-271	190
		TDC-73	7.3	1.58	91.6	710±20	260-395	328
Tunisia	Les Grottes, El Haouaria	GRO-39	3.9	-1.5	109.0	>Modern		
		GRO-76	7.6	-4.5	96.8	264±22	< Cal range	
		GRO-127	12.7	-0.1	94.5	456±23	< Cal range	
		GRO-212	21.2	3.8	93.4	546±26	1-237	119
	*Sidi Mecrhig	SIM-60	6	-3.7	94.9	420±30	< Cal range	
		SIM-71	7.1	0.6	85.5	1260±30	674-855	765
		SIM-145	14.5	-1.5	80.1	1780±30	1222-1360	1291
Greece	Falasma, Crete	Fal-43	4.3	-1.7	110.6	>Modern		
		Fal-55	5.5	-0.3	95.4	380±20	< Cal range	
		Fal-97	9.7	-4.0	93.9	500±20	1-134	68
		Fal-115	11.5	-0.3	93.9	500±20	1-134	68
		Fal-182	18.2	0.4	91.1	745±25	279-422	351
		Fal-230	23	-2.2	93.1	575±20	64-258	161
		Fal-280	28	-1.1	91.9	675±20	150-367	259
Lebanon	Batroun	BAT-41	4.1	-4.7	94.7	440±35	< Cal range	
		BAT-102	10.2	-3.4	76.4	2160±35	1585-1810	1698
	Tripoli	TRI-1 -39	3.9	-1.4	93.7	520±25	1-226	76
		TRI-1 -70	7	-4.9	93.9	505±25	1-147	74
		TRI-1 -119	11.9	-2.0	92.7	610±25	111-280	196
	Tyro	Tyr-F-7	0.7	-5.0	107.5	>Modern		
		Tyr-F-29	2.9	4.2	93.4	545±25	40-236	138
	Sidon	SID-2-20	2	1.1	114.7	>Modern		
		SID-2-35	3.5	0.8	94.6	445±30	< Cal range	
		SID-2-80	8	-0.1	90.3	815±30	315-480	398
		SID-2-109	11	-3.6	90.9	765±30	287-443	365
		SID-2-182	18.2	2.7	93.5	545±30	1-236	119
		SID-1-139	13.9	-1.7	93.7	520±30	1-150	76

607

608

609

610

611